Flow (2021), **1** E10
doi:10.1017/flo.2021.10

FLOW CAMBRIDGE UNIVERSITY PRESS

RESEARCH ARTICLE

Monitoring carbon dioxide to quantify the risk of indoor airborne transmission of COVID-19

Martin Z. Bazant[1,2,*], Ousmane Kodio[2], Alexander E. Cohen[1], Kasim Khan[3], Zongyu Gu[1] and John W.M. Bush[2]

[1]Department of Chemical Engineering, Massachusetts Institute of Technology, Cambridge, MA 02139, USA
[2]Department of Mathematics, Massachusetts Institute of Technology, Cambridge, MA 02139, USA
[3]Independent researcher, USA
*Corresponding author. E-mail: bazant@mit.edu

Received: 4 April 2021; **Revised:** 1 June 2021; **Accepted:** 12 July 2021

Keywords: Respiratory flows; Ventilation; Airborne disease transmission; COVID-19; Carbon dioxide monitoring; Safety guideline

Abstract

A new guideline for mitigating indoor airborne transmission of COVID-19 prescribes a limit on the time spent in a shared space with an infected individual (Bazant & Bush, *Proceedings of the National Academy of Sciences of the United States of America*, vol. 118, issue 17, 2021, e2018995118). Here, we rephrase this safety guideline in terms of occupancy time and mean exhaled carbon dioxide (CO_2) concentration in an indoor space, thereby enabling the use of CO_2 monitors in the risk assessment of airborne transmission of respiratory diseases. While CO_2 concentration is related to airborne pathogen concentration (Rudnick & Milton, *Indoor Air*, vol. 13, issue 3, 2003, pp. 237–245), the guideline developed here accounts for the different physical processes affecting their evolution, such as enhanced pathogen production from vocal activity and pathogen removal via face-mask use, filtration, sedimentation and deactivation. Critically, transmission risk depends on the total infectious dose, so necessarily depends on both the pathogen concentration and exposure time. The transmission risk is also modulated by the fractions of susceptible, infected and immune people within a population, which evolve as the pandemic runs its course. A mathematical model is developed that enables a prediction of airborne transmission risk from real-time CO_2 measurements. Illustrative examples of implementing our guideline are presented using data from CO_2 monitoring in university classrooms and office spaces.

Impact Statement

There is mounting scientific evidence that COVID-19 is primarily transmitted through indoor airborne transmission, as arises when a susceptible person inhales virus-laden aerosol droplets exhaled by an infectious person. A safety guideline to limit indoor airborne transmission (Bazant & Bush, 2021) has recently been derived that complements the public health guidelines on surface cleaning and social distancing. We here recast this safety guideline in terms of total inhaled carbon dioxide (CO_2), as can be readily monitored in most indoor spaces. Our approach paves the way for optimizing air handling systems by balancing health and financial concerns, and so informs policy for safely reopening schools and businesses as the pandemic runs its course. Finally, our approach may be applied quite generally in the mitigation of airborne respiratory illnesses, including influenza.

1. Introduction

Coronavirus disease 2019 (COVID-19) has caused a devastating pandemic since it was first identified in Wuhan, China, in December 2019 (Chen et al., 2020; Li et al., 2020). For over a year, public health guidance has focused on disinfecting surfaces in order to limit transmission through fomites (Van Doremalen et al., 2020) and maintaining social distance in order to limit transmission via large drops generated by coughs and sneezes (Bourouiba, Dehandschoewercker & Bush, 2014; Rosti, Olivieri, Cavaiola, Seminara & Mazzino, 2020). The efficacy of these measures has been increasingly called into question, however, since there is scant evidence for fomite transmission (Gandhi, Yokoe & Havlir, 2020; Lewis, 2021), and large-drop transmission is effectively eliminated by masks (Moghadas et al., 2020).

There is now overwhelming evidence that the pathogen responsible for COVID-19, severe acute respiratory syndrome coronavirus 2 (SARS-CoV-2), is transmitted primarily through exhaled aerosol droplets suspended in indoor air (Bazant & Bush, 2021; Greenhalgh et al., 2021; Jayaweera, Perera, Gunawardana & Manatunge, 2020; Morawska & Cao, 2020; Morawska & Milton, 2020; Prather et al., 2020; Stadnytskyi, Bax, Bax & Anfinrud, 2020; Zhang, Li, Zhang, Wang & Molina, 2020b). Notably, airborne transmission provides the only rational explanation for the so-called 'superspreading events', that have now been well chronicled and all took place indoors (Hamner, 2020; Hwang, Chang, Bumjo & Heo, 2020; Kwon et al., 2020; Miller et al., 2020; Moriarty, 2020; Nishiura et al., 2020; Shen et al., 2020). The dominance of indoor airborne transmission is further supported by the fact that face-mask directives have been more effective in limiting the spread of COVID-19 than either social distancing directives or lockdowns (Stutt, Retkute, Bradley, Gilligan & Colvin, 2020; Zhang et al., 2020b). Indeed, a recent analysis of spreading data from Massachusetts public schools where masking was strictly enforced found no statistically significant effect of social distance restrictions that ranged from three feet to six feet (van den Berg et al., 2021). A recent study of school transmissions in Georgia found that mask use and improvements in ventilation and filtration were the most effective mitigation strategies, while the imposition of barriers or six-foot distancing between desks had little effect (Gettings et al., 2021). Finally, the detection of infectious SARS-CoV-2 virions suspended in hospital room air as far as 5.5 m from an infected patient provides direct evidence for the viability of airborne transmission of COVID-19 (Lednicky et al., 2020; Santarpia et al., 2020).

With a view to informing public health policy, we proceed by developing a quantitative approach to mitigating the indoor airborne transmission of COVID-19, an approach that might be similarly applied to other airborne respiratory diseases. The canonical theoretical framework of Wells (1955) and Riley, Murphy & Riley (1978) describes airborne transmission in an indoor space that is well-mixed by ambient air flows, so that infectious aerosols are uniformly dispersed throughout the space (Beggs, Noakes, Sleigh, Fletcher & Siddiqi, 2003; Gammaitoni & Nucci, 1997; Nicas, Nazaroff & Hubbard, 2005; Noakes, Beggs, Sleigh & Kerr, 2006; Stilianakis & Drossinos, 2010). While exceptions to the well-mixed-room approximation are known to arise (Bhagat, Wykes, Dalziel & Linden (2020); see supplementary information in Bazant & Bush, 2021), supporting evidence for the well-mixed approximation may be found in both theoretical arguments (Bazant & Bush, 2021) and computer simulations of natural and forced convection (Foster & Kinzel, 2021). The Wells–Riley model and its extensions have been applied to a number of superspreading events and used to assess the risk of COVID-19 transmission in a variety of indoor settings (Augenbraun et al., 2020; Buonanno, Morawska & Stabile, 2020a; Buonanno, Stabile & Morawska, 2020b; Evans, 2020; Miller et al., 2020; Prentiss, Chu & Berggren, 2020).

A safety guideline for mitigating indoor airborne transmission of COVID-19 has recently been derived that indicates an upper bound on the cumulative exposure time, that is, the product of the number of occupants and the exposure time (Bazant & Bush, 2021). This bound may be simply expressed in terms of the relevant variables, including the room dimensions, ventilation, air filtration, mask efficiency and respiratory activity. The guideline has been calibrated for COVID-19 using epidemiological data from the best characterized superspreading events and incorporates the measured dependence of expiratory droplet-size distributions on respiratory and vocal activity (Asadi, Bouvier, Wexler & Ristenpart, 2020a;

https://doi.org/10.1017/flo.2021.10 Published online by Cambridge University Press

Asadi et al., 2019; Morawska et al., 2009). An online app has facilitated its widespread use during the pandemic (Khan, Bazant & Bush, 2020). The authors also considered the additional risk of turbulent respiratory plumes and jets (Abkarian, Mendez, Xue, Yang & Stone, 2020a, 2020b), as need be considered when masks are not worn. The accuracy of the guideline is necessarily limited by uncertainties in a number of model parameters, which will presumably be reduced as more data is analysed from indoor spreading events.

Carbon dioxide measurements have been used for decades to quantify airflow and zonal mixing in buildings and so guide the design of heating, ventilation and air-conditioning (known as HVAC) systems (Fisk & De Almeida, 1998; Seppänen, Fisk & Mendell, 1999). Such measurements thus represent a natural source of data for assessing indoor air quality (Corsi, Torres, Sanders & Kinney, 2002), especially as they rely only on relatively inexpensive, widely available CO_2 sensors. Quite generally, high CO_2 levels in indoor settings are known to be associated with poor health and diminished cognitive function (Coley, Greeves & Saxby, 2007; Hung & Derossis, 1989; Salisbury, 1986; Seppänen et al., 1999). MacNaughton et al. (2015) examined the economic and environmental costs of increasing ventilation rates to improve indoor air quality, and concluded that the public health benefits of improved ventilation generally outweigh these costs. Statistically significant correlations between CO_2 levels and illness-related absenteeism in both the work place (Milton, Glencross & Walters, 2000) and classrooms (Mendell et al., 2013; Shendell et al., 2004) have been widely reported (Li et al., 2007). Direct correlations between CO_2 levels and concentration of airborne bacteria have been found in schools (Liu et al., 2000). Correlations between outdoor air exchange rates and respiratory infections in dormitory rooms have also been reported (Bueno de Mesquita, Noakes & Milton, 2020; Sun, Wang, Zhang & Sundell, 2011). Despite the overwhelming evidence of such correlations and the numerous economic analyses that underscore their negative societal impacts (Fisk, 2000; Milton et al., 2000), using CO_2 monitors to make quantitative assessments of the risk of indoor disease transmission is a relatively recent notion (Li et al., 2007).

Rudnick and Milton (2003) first proposed the use of Wells–Riley models, in conjunction with measurements of CO_2 concentration, to assess airborne transmission risk indoors. Their model treats CO_2 concentration as a proxy for infectious aerosols: the two were assumed to be produced proportionally by the exhalation of an infected individual and removed at the same rate by ventilation. The current pandemic has generated considerable interest in using CO_2 monitoring as a tool for risk management of COVID-19 (Bhagat et al., 2020; Hartmann & Kriegel, 2020). The Rudnick–Milton model has recently been extended by Peng and Jimenez (2021) through consideration of the different removal rates of CO_2 and airborne pathogen. They conclude by predicting safe CO_2 levels for COVID-19 transmission in various indoor spaces, which vary by up to two orders of magnitude.

We here develop a safety guideline for limiting indoor airborne transmission of COVID-19 by expressing the safety guideline of Bazant and Bush (2021) in terms of CO_2 concentration. Doing so makes clear that one must limit not only the CO_2 concentration, but also the occupancy time. Our model accounts for the effects of pathogen filtration, sedimentation and deactivation in addition to the variable aerosol production rates associated with different respiratory and vocal activities, all of which alter the relative concentrations of airborne pathogen and CO_2. Our guideline thus quantifies the extent to which safety limits may be extended by mitigation strategies such as mask mandates, air filtration and the imposition of 'quiet spaces'.

In § 2, we rephrase the indoor safety guideline of Bazant and Bush (2021) in terms of the room's CO_2 concentration. In § 3, we present theoretical descriptions of the evolution of CO_2 concentration and infectious aerosol concentration in an indoor space, and highlight the different physical processes influencing the two. We then model the disease transmission dynamics, which allows for the risk of indoor airborne transmission to be assessed from CO_2 measurements taken in real time. In § 4, we apply our model to a pair of data sets tracking the evolution of CO_2 concentration in specific office and classroom settings. These examples illustrate how CO_2 monitoring, when coupled with our safety guideline, provides a means of assessing and mitigating the risk of indoor airborne transmission of respiratory pathogens.

https://doi.org/10.1017/flo.2021.10 Published online by Cambridge University Press

2. Safety guideline for the time-averaged CO_2 concentration

2.1. Occupancy-based safety guideline

We begin by recalling the safety guideline of Bazant and Bush (2021) for limiting indoor airborne disease transmission in a well-mixed space. The guideline would impose an upper bound on the cumulative exposure time,

$$N_t \tau < \frac{\epsilon \bar{\lambda}_c V}{Q_b^2 C_q s_r \bar{p}_m^2}, \tag{1}$$

where N_t is the number of possible transmissions (pairs of infected and susceptible people) and τ is the time in the presence of the infected person(s). The reader is referred to table 1 for a glossary of symbols and their characteristic values. Here Q_b is the mean breathing flow rate and V the room volume. The risk tolerance $\epsilon < 1$ is the prescribed bound on the probability of at least one transmission, as should be chosen judiciously according to the vulnerability of the population (Garg, 2020); for example, Bazant and Bush (2021) suggested $\epsilon = 10\,\%$ for children and 1 % for the elderly.

The only epidemiological parameter in the guideline, C_q, is the infectiousness of exhaled air, measured in units of infection quanta per volume for a given aerosolized pathogen. The notion of 'infection quantum', introduced by Wells (1955), is widely used in epidemiology to measure the expected rate of disease transmission, which may be seen as a transfer of infection quanta between pairs of infected and susceptible individuals. For airborne transmission, a suitable concentration of infection quanta per volume, C_q, can thus be associated with exhaled air without reference to the microscopic pathogen concentration. Notably, C_q is known to depend on the type of respiratory and vocal activity (associated with an individual resting, exercising, speaking, singing, etc.), being larger for the more vigorous activities (Bazant & Bush, 2021; Buonanno et al., 2020b). The relative susceptibility s_r is introduced as a scaling factor for C_q that accounts for differences in the transmissibility of different respiratory pathogens, such as bacteria or viruses (Li et al., 2008; Rudnick & Milton, 2003) with different strains (Davies et al., 2020; Volz et al., 2021), and for differences in the susceptibility of different populations, such as children and adults (Riediker & Morawska, 2020; Zhang et al., 2020a; Zhu et al., 2020).

The mask penetration probability, $p_m(r)$, is a function of drop size that is bounded below by 0 (for the ideal limit of perfect mask filtration) and above by 1 (as is appropriate when no mask is worn). Standard surgical masks at low flow rates allow only 0.04 %–1.5 % of the micron-scale aerosols to penetrate (Chen & Willeke, 1992), but these values should be increased by a factor of 2–10 to account for imperfect fit (Oberg & Brosseau, 2008). Cloth masks show much greater variability (Konda et al., 2020b). The mask penetration probability may also depend on respiratory activity (Asadi et al., 2020b) and direction of airflow (Pan, Harb, Leng & Marr, 2020). Here, for the sake of simplicity, we treat $p_m(r)$ as being constant over the limited aerosol size range of interest, and evaluate $\bar{p}_m = p_m(\bar{r})$ at the effective aerosol radius $\bar{r}$ to be defined below, above which drops tend to settle to the ground faster than they are swept away by ventilation. For this effective aerosol filtration factor, Bazant and Bush (2021) suggested $\bar{p}_m = 1\,\%$–$5\,\%$ for surgical masks (Li et al., 2008; Oberg & Brosseau, 2008), $\bar{p}_m = 10\,\%$–$40\,\%$ for hybrid cloth face coverings and $\bar{p}_m = 40\,\%$–$80\,\%$ for single-layer fabrics (Konda et al., 2020b). Notably, even low quality masks can significantly reduce transmission risk since the bound on cumulative exposure time, (1), scales as $\bar{p}_m^{-2}$.

Finally, we define $\bar{\lambda}_c = \lambda_c(\bar{r})$ as an effective relaxation rate of the infectious aerosol-borne pathogen concentration, $C(r,t)$, evaluated at the effective aerosol radius $\bar{r}$. The size-dependent relaxation rate of the droplet-borne pathogen has four distinct contributions:

$$\lambda_c(r) = \lambda_a + \lambda_f(r) + \lambda_s(r) + \lambda_v(r). \tag{2}$$

Here, λ_a is the ventilation rate, specifically the rate of exchange with outdoor air; $\lambda_f(r) = p_f(r)\lambda_r$ is the filtration rate, where $p_f(r)$ is the droplet removal efficiency for air filtration at a rate λ_r (recirculated air changes per time); $\lambda_s(r) = v_s(r)A/V$ is the net sedimentation rate for infectious droplets with the

https://doi.org/10.1017/flo.2021.10 Published online by Cambridge University Press

Table 1. *Glossary of symbols arising in our theory, their units and characteristics values.*

Symbol	Meaning	Typical Values
Engineering parameters		
N	Number of people, room occupancy	1–1000
τ	Time since an infected person entered the room	0–1000 h
V	Room volume	10–10^4 m^3
A	Floor surface area	5–5000 m^2
H	Mean ceiling height, V/A	2–6 m
Q_a	Ventilation outflow rate	1–10^5 m^3 h^{-1}
λ_a	Ventilation (outdoor air exchange) rate, Q_a/V	0.1–30 h^{-1}
λ_r	Recirculation air exchange rate, Q_r/V	0.1–30 h^{-1}
p_f	Probability of droplet filtration via recirculation	0–1.0
λ_f	Filtration removal rate, $p_f\lambda_r$	0–30 h^{-1}
p_m	Mask penetration probability, $\overline{p}_m = p_m(\overline{r})$	0.01–0.1
Physical parameters		
r	Respiratory drop radius	0.1–100 μm
V_d	Drop volume, $\approx \frac{4}{3}\pi r^3$	10^{-5}–10^6 μm^3
n_d	Drop number density per radius	0.01–1.0 $(cm^3\ \mu m)^{-1}$
v_s	Drop settling speed	10^{-5}–10^2 mm s^{-1}
λ_s	Drop settling rate, $v_s(r)/H$	10^{-5}–10^2 h^{-1}
Q_b	Mean breathing flow rate	0.5–3.0 m^3 h^{-1}
C_0	Background CO_2 concentration	250–450 p.p.m.
C_2	Exhaled CO_2 concentration	0–40 000 p.p.m.
P_2	Production rate of exhaled CO_2	0.02–10 m^3 h^{-1}
Epidemiological parameters		
S, I	Number of susceptible and infected people	
β_a	Airborne transmission rate per infected–susceptible pair	10^{-6}–10 quanta h^{-1}
λ_v	Pathogen (virion) deactivation rate	0.01–10 h^{-1}
λ_c	Pathogen concentration relaxation rate, $\overline{\lambda}_c = \lambda_c(\overline{r})$	0.1–100 h^{-1}
$\bar{r}$	Effective infectious drop radius	0.3–5 μm
P	Pathogen production rate / air volume / drop radius	10^{-6}–10^9 $(h\ \mu m)^{-1}$
C	Infectious pathogen concentration / air volume / radius	10^{-8}–10^4 $(m^3\ \mu m)^{-1}$
c_v	Pathogen (virion) concentration per drop volume	10^4–10^{11} RNA copies mL^{-1}
c_i	Pathogen infectivity, 1/(infectious dose)	0.001–1.0
C_q	Infectiousness of breath, exhaled quanta concentration	1–1000 quanta m^{-3}
λ_q	Quanta emission rate, Q_bC_q	1–1000 quanta h^{-1}
p_i	Probability a person is infected (prevalence)	0–1
p_{im}	Probability a person is immune (by vaccination or exposure)	0–1
p_s	Probability a person is susceptible, $p_s = 1 - p_i - p_{\text{im}}$	0–1
s_r	Relative susceptibility (or transmissibility)	0.1–10
N_t	Expected number of infected–susceptible pairs	0–1000
T_a	Expected number of airborne transmissions, $N_t\langle\beta_a\rangle\tau$	0–100
$\mathcal{R}_{\text{in}}$	Indoor reproductive number, $(N-1)\langle\beta_a\rangle\tau$	0.001–100
ϵ	Risk tolerance, bound on T_a	0.005–0.5

https://doi.org/10.1017/flo.2021.10 Published online by Cambridge University Press

Stokes settling speed $v_s(r)$ sedimenting through a turbulent, well-mixed ambient in a room of height $H = V/A$, volume V and floor area A (Corner & Pendlebury, 1951; Martin & Nokes, 1988); $\lambda_v(r)$ is the deactivation rate of the aerosolized pathogen, which depends weakly on humidity and droplet size (Lin & Marr, 2019; Marr, Tang, Van Mullekom & Lakdawala, 2019; Yang & Marr, 2011), and may be enhanced by other factors such as ultraviolet (UV-C) irradiation (García de Abajo et al., 2020; Hitchman, 2021), chemical disinfectants (Schwartz et al., 2020) or cold plasma release (Filipić, Gutierrez-Aguirre, Primc, Mozetič & Dobnik, 2020; Lai, Cheung, Wong & Li, 2016).

Notably, only the first of the four removal rates enumerated in (2) is relevant in the evolution of CO_2; thus, the concentrations of CO_2 and airborne pathogen may evolve independently. Specifically, the proportionality between the two equilibrium concentrations varies in different indoor settings (Peng & Jimenez, 2021), for example in response to room filtration (Hartmann & Kriegel, 2020). Moreover, when transient effects arise, for example, following the arrival of an infectious individual or the opening of a window, the two concentrations adjust at different rates. Finally, we note that there may also be sources of CO_2 other than human respiration, such as emissions from animals, stoves, furnaces, fireplaces or carbonated drinks, as well as sinks of CO_2, such as plants, construction materials or pools of water, which we neglect for simplicity. As such, following Rudnick and Milton (2003), we assume that the primary source of excess CO_2 is exhalation by the human occupants of the indoor space.

In order to prevent the growth of an epidemic, the safety guideline should bound the indoor reproductive number, $\mathcal{R}_{\text{in}}$, which is the expected number of transmissions if an infectious person enters a room full of susceptible people. Indeed, the safety guideline, (1), corresponds to the bound $\mathcal{R}_{\text{in}} < \epsilon$ with the choice $N_t = N - 1$, and so would limit to ϵ the risk of an infected person entering the room of occupancy N transmitting to any other person during the exposure time τ. If the epidemic is well underway or subsiding, the guideline should take into account the prevalence of infection p_i and immunity p_{im} (as achieved by previous exposure or vaccination) in the local population. Assuming a trinomial distribution of N people who are infected, immune or susceptible, with mutually exclusive probabilities p_i, p_{im} and $p_s = 1 - p_i - p_{\text{im}}$, respectively, the expected number of infected–susceptible pairs is $N(N-1)p_ip_s$. It is natural to switch between these two limits ($N_t = N - 1$ and $N_t = N(N-1)p_ip_s$) when one infected person is expected to be in the room, $Np_i = 1$, and thus set

$$N_t = (N-1)\min\{1, Np_i(1 - p_i - p_{\text{im}})\}. \tag{3}$$

One may thus account for the changing infection prevalence p_i and increasing immunity p_{im} in the local population as the pandemic evolves.

2.2. *CO_2-based safety guideline*

The outdoor CO_2 concentration is typically in the range $C_0 = 350$–450 p.p.m., with higher values in urban environments (Prill et al., 2000) and lower values in forests (Higuchi, Worthy, Chan & Shashkov, 2003). In the absence of other indoor CO_2 sources, human occupancy in poorly ventilated spaces can lead to CO_2 levels of several thousand p.p.m. People have reported headaches, slight nausea, drowsiness and diminished decision-making performance for levels above 1000 p.p.m. (Fisk, Satish, Mendell, Hotchi & Sullivan, 2013; Krawczyk, Rodero, Gładyszewska-Fiedoruk & Gajewski, 2016), while short exposures to much higher levels may go unnoticed. As an example of CO_2 limits in industry, the American Conference of Governmental Industrial Hygienists recommends a limit of 5000 p.p.m. for an eight-hour period and 30 000 p.p.m. for 10 min. A value of 40 000 p.p.m. is considered to be immediately life-threatening.

We denote by C_0 the background concentration that would arise in the room at zero occupancy, and by C_2 the excess CO_2 concentration (relative to C_0) associated with human respiration. The total rate of CO_2 production by respiration in the room is given by $P_2 = NQ_bC_{2,b}$, where $C_{2,b}$ is the CO_2 concentration of exhaled air, approximately $C_{2,b} = 38\,000$ p.p.m., although the net CO_2 production rate, $Q_bC_{2,b}$ varies considerably with body mass and physical activity (Persily & de Jonge, 2017). If the

https://doi.org/10.1017/flo.2021.10 Published online by Cambridge University Press

production rate P_2 and the ventilation flow rate $Q = \lambda_a V$ are constant, then the steady-state value of the excess CO_2 concentration,

$$C_{2,s} = \frac{P_2}{Q} = \frac{Q_b C_{2,b} N}{\lambda_a V}, \tag{4}$$

is simply the ratio of the individual CO_2 flow rate, $Q_b C_{2,b}$, and the ventilation flow rate per person, Q/N.

The safety guideline, (1), was derived on the basis of the conservative assumption that the infectious aerosol concentration has reached its maximum, steady-state value. If we assume, for consistency, that the CO_2 concentration has done likewise, and so approached the value expressed in (4), then the guideline can be recast as a bound on the safe mean excess CO_2 concentration,

$$\langle C_2 \rangle \tau = \int_0^\tau C_2 \, \mathrm{d}t < \frac{\epsilon C_{2,b}}{\lambda_q s_r \overline{p}_m^2} \frac{\overline{\lambda}_c}{\lambda_a} \frac{N}{N_t}, \tag{5}$$

where we replace the steady excess CO_2 concentration with its time average, $\langle C_2 \rangle \approx C_{2,s}$, and define the mean quanta emission rate per infected person, $\lambda_q = Q_b C_q$. For the early to middle stages of an epidemic or when p_i and p_{im} are not known, we recommend setting $N/N_t = 1 < N/(N-1) \approx 1$, for a conservative CO_2 bound that limits the indoor reproductive number. In the later stages of an epidemic, as the population approaches herd immunity ($p_i \to 0$, $p_{\mathrm{im}} \to 1$), the safe CO_2 bound diverges, $N/N_t \to \infty$, and so may be supplanted by the limits on CO_2 toxicity noted above, that lie in the range 5000–30 000 p.p.m. for eight hour and 10 minute exposures, respectively. Our simple CO_2-based safety guideline, (5), reveals scaling laws for exposure time, filtration, mask use, infection prevalence and immunity, factors that are not accounted for by directives that would simply impose a limit on CO_2 concentration. The substantial increase in safe occupancy times, as one proceeds from the peak to the late stages of the pandemic, is evident in the difference between the solid and dashed lines in figure 1, which were evaluated for the case of a typical classroom in the USA (Bazant & Bush, 2021). This example shows the critical role of exposure time in determining the safe CO_2 level, a limit that can be increased dramatically by efficient mask use and to a lesser extent by filtration. When infection prevalence p_i falls below 10 per 100 000 (an arbitrarily chosen small value), the chance of transmission is extremely low, allowing for long occupancy times. The risk of transmission at higher levels of prevalence, as may be deduced by interpolating between the solid and dashed lines in figure 1, could also be rationally managed by monitoring the CO_2 concentration and adhering to the guideline.

3. Mathematical model of CO_2 monitoring to predict airborne disease transmission risk

3.1. CO_2 dynamics

We follow the traditional approach of modelling gas dynamics in a well-mixed room (Shair & Heitner, 1974), as a continuous stirred tank reactor (Davis & Davis, 2012). Given the time dependence of occupancy, $N(t)$, mean breathing flow rate, $Q_b(t)$, and ventilation flow rate, $Q_a(t) = \lambda_a(t) V$, one may express the evolution of the excess CO_2 concentration $C_2(t)$ in a well-mixed room through

$$V \frac{\mathrm{d}C_2}{\mathrm{d}t} = P_2(t) - Q_a(t) C_2, \tag{6}$$

where

$$P_2(t) = N(t) Q_b(t) C_{2,b} \tag{7}$$

is the exhaled CO_2 production rate. The relaxation rate for excess CO_2 in response to changes in $P_2(t)$ is precisely equal to the ventilation rate, $\lambda_a(t) = Q_a(t)/V$. For constant λ_a, the general solution of (6)

https://doi.org/10.1017/flo.2021.10 Published online by Cambridge University Press

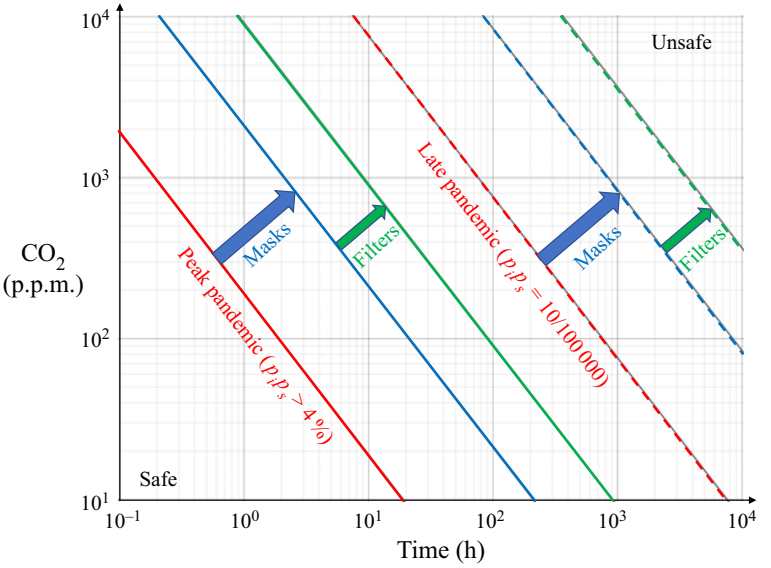

Figure 1. *Illustration of the safety guideline, (5), which bounds the safe excess CO_2 (p.p.m.) and exposure time τ (hours). Here, we consider the case of a standard US classroom (with an area of 83.6 m^2 and a ceiling height of 3.6 m) with $N = 25$ occupants, assumed to be children engaging in normal speech and light activity ($\lambda_q s_r = 30$ quanta h^{-1}) with moderate risk tolerance ($\epsilon = 10$ %). Comparison with the most restrictive bound on the indoor reproductive number without any precautions (red line) indicates that the safe CO_2 level or occupancy time is increased by at least an order of magnitude by the use of face masks (blue line), even with relatively inconsistent use of cloth masks ($p_m = 30$ %). The effect of air filtration (green line) is relatively small, shown here for a case of efficient HEPA filtration ($p_f = 99$ %) with 17 % outdoor air fraction ($\lambda_f = 5\lambda_a$). All three bounds are increased by several orders of magnitude (dashed lines) during late pandemic conditions ($p_i p_s = 10$ per 100 000), when it becomes increasingly unlikely to find an infected–susceptible pair in the room. The other parameters satisfy $(\lambda_v+\lambda_s)/\lambda_a = 0.5$, as could correspond to, for example, $\lambda_v = 0.3$, $\lambda_s = 0.2$ and $\lambda_a = 1$ h^{-1} (1 ACH).*

for $C_2(0) = 0$ is given by

$$C_2(t) = \int_0^t \exp(-\lambda_a(t-t'))\frac{P_2(t')}{V}\mathrm{d}t', \tag{8}$$

which can be derived by Laplace transform or using an integrating factor. The time-averaged excess CO_2 concentration can be expressed as

$$\langle C_2\rangle = \frac{1}{\tau}\int_0^\tau (1-\exp(-\lambda_a(\tau-t)))\,\frac{P_2(t)}{Q_a}\mathrm{d}t \tag{9}$$

by switching the order of time integration. If $P_2(t)$ is slowly varying over the ventilation time scale λ_a^{-1}, the time-averaged CO_2 concentration may be approximated as

$$\langle C_2\rangle \approx \frac{\langle P_2\rangle}{Q_a} - \left(\frac{1-\mathrm{e}^{-\lambda_a\tau}}{\lambda_a\tau}\right)\frac{P_2(\tau)}{Q_a}, \tag{10}$$

where the excess CO_2 concentration approaches the ratio of the mean exhaled CO_2 production rate to the ventilation flow rate at long times, $\tau \gg \lambda_a^{-1}$, as indicated in (4).

https://doi.org/10.1017/flo.2021.10 Published online by Cambridge University Press

3.2. Infectious aerosol dynamics

Following Bazant and Bush (2021), we assume that the radius-resolved concentration of infectious aerosol-borne pathogen, $C(r,t)$, evolves according to

$$V\frac{\partial C}{\partial t} = P(r,t) - \lambda_c(r,t)VC, \tag{11}$$

where the mean production rate,

$$P(r,t) = I(t)Q_b(t)n_d(r,t)V_d(r)p_m(r)c_v(r), \tag{12}$$

depends on the number of infected people in the room, $I(t)$, and the size distribution $n_d(r,t)$ of exhaled droplets of volume $V_d(r)$ containing a pathogen (i.e. virion) at microscopic concentration, $c_v(r)$. The droplet size distribution is known to depend on expiratory and vocal activity (Asadi et al., 2019, 2020c; Morawska et al., 2009). Quite generally, the aerosols evolve according to a dynamic sorting process (Bazant & Bush, 2021): the drop-size distribution evolves with time until an equilibrium distribution obtains.

Given the time evolution of excess CO_2 concentration, $C_2(t)$, one may deduce the radius-resolved pathogen concentration $C(r,t)$ by integrating the coupled differential equation

$$\frac{\partial C}{\partial t} + \lambda_c(r,t)C = \frac{P(r,t)}{P_2(t)}\left(\frac{\mathrm{d}C_2}{\mathrm{d}t} + \lambda_a(t)C_2\right). \tag{13}$$

This integration can be done numerically or analytically via Laplace transform or integrating factors if one assumes that λ_a, λ_c, P and P_2 all vary slowly over the ventilation (air change) time scale, λ_a^{-1}. In that case, the general solution takes the form

$$C(r,t) \approx \frac{P}{P_2}\left(C_2(t) + (\lambda_a - \lambda_c(r))\int_0^t \exp(-\lambda_c(r)(t-t'))C_2(t')\,\mathrm{d}t'\right), \tag{14}$$

where we consider the infectious aerosol build-up from $C(r,0) = 0$.

3.3. Disease transmission dynamics

According to Markov's inequality, the probability of at least one airborne transmission taking place during the exposure time τ is bounded above by the expected number of airborne transmissions, $T_a(\tau)$, and the two become equal in the (typical) limit of rare transmissions, $T_a(\tau) \ll 1$. The expected number of transmissions to $S(t)$ susceptible people is obtained by integrating the mask-filtered inhalation rate of infection quanta over both droplet radius and time:

$$T_a(\tau) = \int_0^\tau S(t)Q_b(t)s_r\left(\int_0^\infty C(r,t)c_i(r)p_m(r)\,\mathrm{d}r\right)\mathrm{d}t, \tag{15}$$

where $c_i(r)$ is the infectivity of the aerosolized pathogen. The infectivity is measured in units of infection quanta per pathogen and generally depends on droplet size. One might expect pathogens contained in smaller aerosol droplets with $r < 5$ μm to be more infectious than those in larger drops, as reported by Santarpia et al. (2020) for SARS-CoV-2, on the grounds that smaller drops more easily penetrate the respiratory tract, absorb and coalesce onto exposed tissues, and allow pathogens to escape more quickly by diffusion to infect target cells. The mask penetration probability $p_m(r)$ also decreases rapidly with increasing drop size above the aerosol range for most filtration materials (Chen & Willeke, 1992; Konda et al., 2020b; Li et al., 2008; Oberg & Brosseau, 2008), so the integration over all radii in (15) gives the most weight to the aerosol size range, roughly $r < 5$ μm. We note that this range includes the maxima in exhaled droplet size distributions (Asadi et al., 2019, 2020c; Morawska et al., 2009) as defined in

https://doi.org/10.1017/flo.2021.10 Published online by Cambridge University Press

terms of either number or total volume in the aerosol range (Bazant & Bush, 2021); nevertheless, larger droplets may also contribute to airborne transmission (Tang et al., 2021).

The inverse of the infectivity, c_i^{-1}, is equal to the 'infectious dose' of pathogens from inhaled aerosol droplets that would cause infection with probability $1-(1/e)=63\,\%$. Bazant and Bush (2021) estimated the infectious dose for SARS-CoV-2 to be of the order of 10 aerosol-borne virions. Notably, the corresponding infectivity, $c_i \sim 0.1$, is an order of magnitude larger than previous estimates for SARS-CoV (Buonanno et al., 2020b; Watanabe, Bartrand, Weir, Omura & Haas, 2010), which is consistent with only COVID-19 reaching pandemic status. The infectivity is known to vary across different age groups and pathogen strains, a variability that is captured by the relative susceptibility, s_r. For example, Bazant and Bush (2021) suggest assigning $s_r = 1$ for the elderly (over 65 years old), $s_r = 0.68$ for adults (aged 15–64) and $s_r = 0.23$ for children (aged 0–14) for the original Wuhan strain of SARS-CoV-2, based on a study of transmission in quarantined households in China (Zhang et al., 2020a). The authors further suggested multiplying these values by 1.6 for the more infectious Alpha variant of concern of the lineage B.1.1.7 (VOC 202012/01), which emerged in the UK with a reproductive number that was 60 % larger than that of the original strain (Davies et al., 2020; Volz et al., 2021). Based on the latest epidemiological data (Abdool Karim & de Oliveira, 2021), we likewise suggest multiplying s_r by 1.5 for the South African variant, 501 Y.V2, and by 1.2 for the Californian variants, B.1.427 and B.1.429. Appropriate factors multiplying s_r for more recent strains are provided on our online app (Khan, Bazant & Bush, 2020), such as 1.5 for the Beta variant B.1.351 from South Africa, 2.0 for the Gamma variant P.1 from Brazil and 2.5 for the Delta variant B.1.617.2 from India that has become dominant at the time of publication.

3.4. Approximate formula for the airborne transmission risk from CO_2 measurements

Equations (14) and (15) provide an approximate solution to the full model that depends on the exhaled droplet size distribution, $n_d(r,t)$, and mean breathing rate, $Q_b(t)$, of the population in the room. Since the droplet distributions $n_d(r)$ have only been characterized in certain idealized experimental conditions (Asadi et al., 2020a, 2020c; Morawska et al., 2009), it is useful to integrate over r to obtain a simpler model that can be directly calibrated for different modes of respiration using epidemiological data (Bazant & Bush, 2021). Assuming $Q_b(t)$, $I(t)$, $S(t)$, $N(t)$ and $n_d(r,t)$ vary slowly over the relaxation time $\overline{\lambda_c}^{-1}$, we may substitute (14) into (15) and perform the time integral of the second term to obtain

$$T_a(\tau) \approx \frac{s_r \lambda_a}{C_{2,b}} \int_0^\tau \int_0^\infty \frac{n_q(r,t) p_m(r)^2}{\lambda_c(r)} \frac{Q_b(t) I(t) S(t) C_2(t)}{N(t)} \left[1 + \left(\frac{\lambda_c(r)}{\lambda_a} - 1\right) \exp(-\lambda_c(r)(\tau - t))\right] \mathrm{d}r\, \mathrm{d}t, \tag{16}$$

where $n_q(r,t) = n_d(r,t) V_d(r) c_v(r) c_i(r)$ is the radius-resolved exhaled quanta concentration.

Following Bazant and Bush (2021), we define an effective radius of infectious aerosols $\bar{r}$ such that

$$\int_0^\infty \frac{n_q(r,t) p_m(r)^2}{\lambda_c(r)} \mathrm{d}r \equiv \frac{C_q(t) p_m(\bar{r})^2}{\lambda_c(\bar{r})}, \tag{17}$$

where $C_q(t) = \int_0^\infty n_q(r,t)\, \mathrm{d}r$ is the exhaled quanta concentration, which may vary in time with changes in expiratory activity, for example, following a transition from nose breathing to speaking. In principle, the effective radius $\bar{r}$ can be evaluated, given a complete knowledge of the dependence on drop radius of the mask penetration probability, $p_m(r)$, and of all the factors that determine the exhaled quanta concentration, $n_q(r,t)$ and pathogen removal rate, $\lambda_c(r)$. While these dependencies are not readily characterized, typical values of $\bar{r}$ are at the scale of several microns, based on the size dependencies of $n_d(r,t)$, $c_i(r)$ and $p_m(r)$ noted above.

Further simplifications allow us to derive a formula relating CO_2 measurements to transmission risk. By assuming that $C_q(t)$ varies slowly over the time scale of concentration relaxation, one may

https://doi.org/10.1017/flo.2021.10 Published online by Cambridge University Press

approximate the memory integral with the same effective radius $\overline{r}$. Thus, accounting for immunity and infection prevalence in the population via

$$\frac{I(t)S(t)}{N(t)} \approx \frac{N_t}{N} = \left(1 - \frac{1}{N}\right) \min\{1, Np_i p_s\}, \tag{18}$$

we obtain a formula for the expected number of airborne transmissions,

$$T_a(\tau) \approx \frac{s_r \overline{p}_m^2}{C_{2,b}} \frac{\lambda_a}{\overline{\lambda}_c} \frac{N_t}{N} \int_0^\tau \lambda_q(t) C_2(t) \left[1 + \left(\frac{\overline{\lambda}_c}{\lambda_a} - 1\right) \exp(-\overline{\lambda}_c(\tau - t))\right] \mathrm{d}t, \tag{19}$$

in terms of the excess CO_2 time series, $C_2(t)$, where $\lambda_q(t) = C_q(t)Q_b(t)$ is the mean quanta emission rate. It is also useful to define the expected transmission rate,

$$\frac{\mathrm{d}T_a}{\mathrm{d}t}(\tau) = N_t \beta_a(\tau) = \frac{s_r \overline{p}_m^2}{C_{2,b}} \frac{\lambda_a}{\overline{\lambda}_c} \frac{N_t}{N} \left[\lambda_q(\tau) C_2(\tau) + (\lambda_a - \overline{\lambda}_c) \int_0^\tau \lambda_q(t) C_2(t) \exp(-\overline{\lambda}_c(\tau - t))\, \mathrm{d}t\right], \tag{20}$$

which allows for direct assessment of airborne transmission risk based on CO_2 levels. A pair of examples of such assessments will be presented in § 4.

Notably, the mean airborne transmission rate expected per infected–susceptible pair, $\beta_a(t)$, reflects the environment's memory of the recent past, which persists over the pathogen relaxation time scale, $\overline{\lambda}_c^{-1}$. Likewise, the CO_2 concentration defined in (9) has a memory of recent changes in CO_2 sources or ventilation, which persists over the air change time scale. Notably, the airborne pathogen concentration equilibrates more rapidly than CO_2; specifically, $\lambda_a^{-1} > \overline{\lambda}_c^{-1}$, since CO_2 is unaffected by the filtration, sedimentation and deactivation rates enumerated in (2). The time delays between the production of CO_2 and infectious aerosols by exhalation and their build-up in the well-mixed air of a room shows that CO_2 variation and airborne transmission are inherently non-Markovian stochastic processes. As such, any attempt to predict fluctuations in airborne transmission risk would require stochastic generalizations of the differential equations governing the mean variables, (6) and (11), and so represent a stochastic formulation of the Wells–Riley model (Noakes & Sleigh, 2009).

3.5. Reduction to the CO_2-based safety guideline

Finally, we connect the general result, (19), with the CO_2-based safety guideline derived above, (5). Since $C_2(t)$ varies on the ventilation time scale λ_a^{-1}, which is necessarily longer than the relaxation time scale of the infectious aerosols $\overline{\lambda}_c^{-1}$, we may assume that $\lambda_q(t)C_2(t)$ is slowly varying and evaluate the integral in (19). We thus arrive at the approximation

$$T_a(\tau) \approx \frac{s_r \overline{p}_m^2}{C_{2,b}} \frac{\lambda_a}{\overline{\lambda}_c} \frac{N_t}{N} \left[\langle \lambda_q C_2 \rangle \tau + \frac{\lambda_q(\tau) C_2(\tau)}{\overline{\lambda}_c} \left(\frac{\overline{\lambda}_c}{\lambda_a} - 1 + \mathrm{e}^{-\overline{\lambda}_c \tau}\right)\right]. \tag{21}$$

Since $\lambda_q(t)C_2(t)$ is slowly varying, the second term in brackets is negligible relative to the first for times longer than the ventilation time, $\tau \gg \lambda_a^{-1} > \overline{\lambda}_c^{-1}$. In this limit, the imposed bound on expected transmissions, $T_a(\tau) < \epsilon$, is approximated by

$$\langle \lambda_q C_2 \rangle \tau = \int_0^\tau \lambda_q(t) C_2(t)\, \mathrm{d}t < \frac{\epsilon C_{2,b}}{s_r \overline{p}_m^2} \frac{\overline{\lambda}_c}{\lambda_a} \frac{N}{N_t}. \tag{22}$$

This formula reduces to the safety guideline, (5), in the limit of constant mean quanta emission rate, λ_q, which confirms the consistency of our assumptions.

https://doi.org/10.1017/flo.2021.10 Published online by Cambridge University Press

4. Examples of implementation

We proceed by illustrating the process by which the guideline, (5), can be coupled to real data obtained from CO_2 monitors. Specifically, we consider time series of CO_2 concentration gathered in classroom and office settings at the Massachusetts Institute of Technology using an Atlas Scientific EZO-CO2 Embedded NDIR CO2 Sensor controlled with an Arduino Uno and an Aranet4, respectively. The measurements were collected at desk level. Social distancing guidelines were adhered to, and masks were worn by all participants. We assume a constant exhaled CO_2 concentration of 38 000 p.p.m., and use the global minimum of the CO_2 series as the background CO_2 level C_0 from which the excess concentration $C_2(t)$ was deduced. Notably, the relatively small fluctuations in the CO_2 measurements recorded in a variety of settings support the notion of a well-mixed room.

The sensors yield a time series of CO_2 concentration that we use, along with (19) and (20), to calculate the transmission rate, assuming that there is a single infected person in the room and that all others are susceptible ($N_t = N - 1$). In this case, the expected number of transmissions is equal to the indoor reproductive number, $T_a(\tau) = \mathcal{R}_{\text{in}}(\tau)$, and the transmission rate is $(\mathrm{d}T_a/\mathrm{d}t)(\tau) = N_t\beta_a(\tau)$. The approximations made in the derivation above are valid in these examples, so a direct numerical solution of (13) would yield an identical result. In particular, the 'slowly varying' assumptions are satisfied, since we keep N and I constant, and any time-dependence of Q_b cancels in the ratio P/P_2. Moreover, there was no indication that the air change rate varied over the relatively short time periods considered. Finally, the droplet distributions $n_d(r, t)$ may vary in time, but no significant changes in mean respiratory activity were observed or evidenced in the CO_2 measurements.

We choose realistic values of the parameters that fall within the typical ranges estimated by Bazant and Bush (2021). The mean breathing rate is set to a value, $Q_b = 0.5\ \mathrm{m^3\ h^{-1}}$, appropriate for light respiratory activity, and we choose an effective settling speed of $\overline{v}_s = 0.108\ \mathrm{m\ h^{-1}}$ appropriate for $\bar{r} = 0.5\ \mu\mathrm{m}$. Larger values of Q_b would be appropriate for more vigorous respiratory activity, as would accompany, for example, a workout at a gym. Our estimate for $\overline{v}_s$ may be revised in response to additional information concerning the dependence on size of the infectivity of exhaled aerosol droplets (Stadnytskyi et al., 2020). The viral deactivation rate for SARS-CoV-2 is set to $\lambda_v = 0.3\ \mathrm{h^{-1}}$, an estimate appropriate for 50 % relative humidity. We plot $N_t\beta_a(\tau)$ and $\mathcal{R}_{\text{in}}(\tau)$ for cases where masks are and are not worn, and choose a mask penetration probability of $p_m \approx 0.3$, as is roughly appropriate for a cloth mask (Konda et al., 2020a). For more effective masks, such as surgical masks or N95s, a smaller p_m value is appropriate, as noted above. The parameters $\overline{\lambda}_c$, λ_a, H and N are chosen according to the specific scenario presented. Exhaled COVID-19 quanta concentrations C_q for various expiratory activities are estimated from figure 2 of Bazant and Bush (2021). In order to be conservative, we assume that $s_r = 1$, suitable for the most susceptible individuals exposed to the Wuhan strain of SARS-CoV-2. When applying our model to less susceptible populations, such as children (Zhang et al., 2020a; Zhu et al., 2020) or vaccinated individuals exposed to new variants (Sheikh et al., 2021; Nasreen et al., 2021), a smaller s_r value may be used.

4.1. Small office with two workers

Figure 2a shows CO_2 measurements taken in an office of length $L = 4.2$ m, width $W = 3$ m and height $H = 3$ m. Initially, a single worker is present, but at 19:00, a second worker arrives at the office. The workers exit the office at 21:09, return at 21:39 and exit again at 22:30. As the participants were speaking, we use $C_q = 72\ \mathrm{quanta\ m^{-3}}$ (Bazant & Bush, 2021). We compute the room's ventilation rate, $\lambda_a \approx 2.3\ \mathrm{h^{-1}}$, from the exponential relaxation that follows the occupants' exit from the office (as indicated by the orange curve in figure 2). The office was equipped with moderate ventilation, which we characterize with $p_f = 0.99$ and $\lambda_r = 6\ \mathrm{h^{-1}}$. The background concentration $C_0 = 420$ p.p.m. is evident both before and after occupancy.

https://doi.org/10.1017/flo.2021.10 Published online by Cambridge University Press

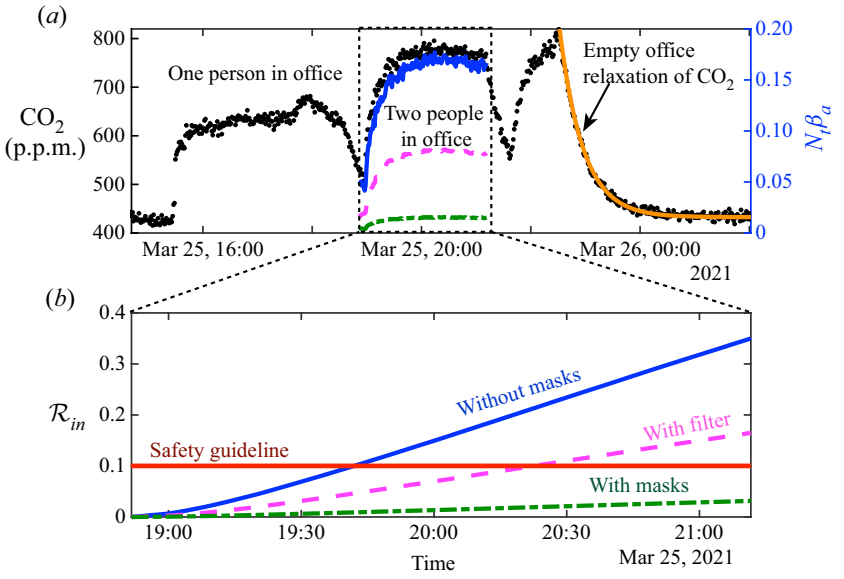

Figure 2. *Measured CO_2 concentration and calculated transmission rate in a two-person office. (a) Black dots represent the concentration of CO_2. The solid blue, dashed magenta and dash–dot green curves represents the transmission rate, as calculated from (20) for three different scenarios, two of which were hypothetical: (blue) the pair are not wearing masks and there is no filtration present; (magenta) the pair are not wearing masks and there is filtration present; (green) the pair are wearing masks and there is no filtration present. The orange solid curve denotes the period of exponential relaxation following the exit of the room's occupants, from which one may infer both the room's ventilation rate, $\lambda_a = 2.3\ h^{-1}$, and the background CO_2 concentration, $C_0 = 420$ p.p.m. (b) Corresponding blue, magenta and green curves, deduced by integrating (20), indicate the total risk of transmission over the time of shared occupancy. If the pair were not wearing masks, the safety limit $\mathcal{R}_{in} < 0.1$ would be violated after approximately an hour.*

As shown in figure 2b, if the office workers were not wearing masks, the safety guideline of expected transmissions $T_a < 10\,\%$ would be violated after approximately an hour together. However, office workers wearing cloth masks would not violate the safety guideline during the 2.5 h spent together. Filtration without masks also extends the occupancy time limits; however, $\mathcal{R}_{\text{in}}$ approaches the safety limit after approximately 2 h. While this example should not be taken as a definitive statement of danger or safety in this setting, it does serves to illustrate how our CO_2 guideline can be implemented in a real-life situation.

4.2. University classroom adhering to social distancing guidelines

We next monitor CO_2 levels during a university lecture. There were $N = 12$ participants in a lecture hall of length $L = 13$ m, width $W = 12$ m and height $H = 3$ m. The lecture started at 13:05 and finished at 13:50. Four people remained in the room for 30 min after the class. The classroom has mechanical ventilation, which is characterized in terms of $\lambda_a \approx 5.2\ h^{-1}$ (corresponding to a 12 min outdoor air change time; here, we estimate λ_a by fitting the build-up of CO_2, see figure 3). During the lecture, the professor spoke while the students were quiet and sedentary; thus, we assume $C_q = 30$ quanta m^{-3} (Bazant & Bush, 2021). The maximum CO_2 concentration reached in the classroom was ≈550 p.p.m., the excess level no more than 100 p.p.m. Thus, the safety limit was never exceeded, and would not have been even if masks had not been worn. We note that this lecture hall was particularly large, well-ventilated and sparsely populated, and so should not be taken as being representative of a classroom setting. A more complete assessment of safety in schools would require integrating CO_2

https://doi.org/10.1017/flo.2021.10 Published online by Cambridge University Press

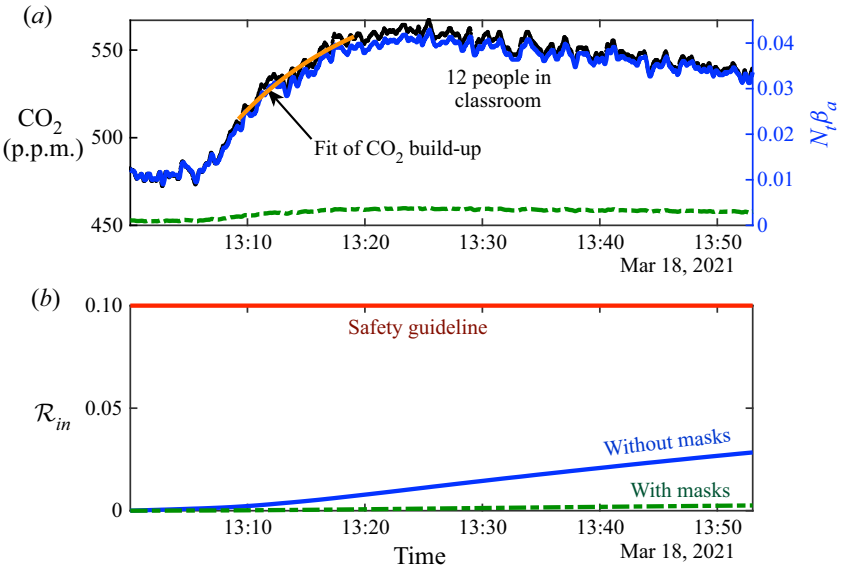

Figure 3. *Measured CO_2 concentration and calculated transmission rate for 12 masked students in a university lecture hall. (a) Black dots represent the concentration of CO_2. The dash–dot green and solid blue curves represent the transmission rate, as calculated from (20), when the occupants are wearing masks, and in the hypothetical case where they are not, respectively. The gold curve indicates a fit to the transient build-up of CO_2 from which we infer an air change rate of $\lambda_a = 5.2/h$. (b) The dash–dot green and solid blue curves indicate the total risk of transmission with and without masks, respectively, as deduced by integrating (20) over time. Even had masks not been worn, the safety guideline would not have been violated during the lecture.*

concentrations over a considerably longer time interval. For example, if students are tested weekly for COVID-19, then one should assess the mean CO_2 concentration in class during the course of an entire school week. Nevertheless, this second example further illustrates the manner in which our model may be applied to real-world settings and suggests that precautions such as ventilation, filtration and mask use, can substantially increase safe occupancy times.

5. Conclusion

Mounting evidence suggests that COVID-19 is spread primarily via indoor airborne transmission. Such an inference is no surprise, as such is also the case for many other respiratory illnesses, including influenza, tuberculosis, measles and severe acute respiratory syndrome (as is caused by a precursor to SARS-CoV-2, the coronavirus SARS-CoV). More than a year into the pandemic, public health guidance continues to emphasize the importance of social distancing and surface cleaning, despite evidence that mask directives are much more effective than either in limiting airborne transmission. We have here illustrated the manner in which CO_2 monitoring may be used in conjunction with the safety guideline of Bazant and Bush (2021) to assess the risk of indoor airborne respiratory disease transmission, including that of COVID-19. Morawska et al. (2021) emphasize the need for improved air quality standards to combat airborne respiratory diseases, similar in spirit to food safety standards for restaurants. We hope that our study might prove useful in defining such standards, and in informing personal and policy decisions about closing and reopening indoor spaces, such as schools and businesses.

We have here reformulated the COVID-19 indoor safety guideline of Bazant and Bush (2021), expressing it in terms of cumulative exposure to CO_2, which can be readily monitored in real time for most indoor spaces. In so doing, we have built upon the seminal work of Rudnick and Milton (2003), as was recently extended and applied to COVID-19 by Peng and Jimenez (2021). The guideline of Bazant

https://doi.org/10.1017/flo.2021.10 Published online by Cambridge University Press

and Bush (2021) makes clear that, since the risk of indoor airborne infection is determined by the total volume of pathogen inhaled, safety limits intended to protect against it must be expressed in terms of occupancy time. Likewise, in the context of CO_2 measurements, safety limits cannot be expressed solely in terms of a limit on CO_2 levels, but must also depend on occupancy time. As we have demonstrated with our two case studies, the safety guideline, (5), when coupled with CO_2 monitors, allows for real-time assessment of risk of airborne disease transmission $\mathcal{R}_{in}$ in indoor spaces. Moreover, this approach has the distinct advantage that one can assess certain key model parameters, including the background concentration of CO_2 and the room's ventilation rate, directly from the CO_2 measurements.

Within a well-mixed space, CO_2 is effectively a passive scalar that tracks the ambient flow, and is removed only through exchange with outdoor air. Aerosol-borne pathogens are subject to additional removal mechanisms, including filtration (by face masks and internal circulation), sedimentation and deactivation. Thus, the concentration of CO_2 cannot be taken as a proxy for those of an aerosol-borne pathogen without resolving the proportionality constant between the two that results from these additional removal mechanisms. We stress that the effects of face mask use are dramatic in reducing the ratio of aerosol-borne pathogens to CO_2 concentration, and in reducing the risk of indoor transmission. Finally, we note that the additional removal mechanisms acting on the droplet-borne pathogen alter not only its equilibrium concentrations relative to that of CO_2, but their relaxation times in transient situations, as may be treated using the mathematical formalism of Bazant and Bush (2021).

We emphasize that the caveats enumerated by Bazant and Bush (2021) concerning the limitations of their safety guideline apply similarly here. First, there is considerable uncertainty in a number of model parameters, including the critical viral load and relative susceptibility. While our inferences are consistent with available data, we hope that these uncertainties will be reduced as more COVID-19 spreading events are characterized and analysed. Second, when masks are not worn, there is substantial additional risk of short-range airborne transmission from respiratory jets and plumes, as accompany breathing, speaking (Abkarian et al., 2020a; Abkarian & Stone, 2020), coughing and sneezing (Bourouiba et al., 2014). Third, while the assumption of the well-mixed room is widely applied and represents a reasonable first approximation, it is known to have limitations (Bhagat et al., 2020; Linden, Lane-Serff & Smeed, 1990; Linden, 1999). Notably, measured fluctuations in CO_2 levels provide a direct means of assessing the validity of the well-mixed-room hypothesis, especially when several sensors are used simultaneously at different locations in the same space. Indeed, CO_2 monitoring has been used for decades to assess the quality of air handling and zonal mixing in buildings (Cheng et al., 2011; Fisk & De Almeida, 1998; Hung & Derossis, 1989; Salisbury, 1986; Seppänen et al., 1999), and can now be repurposed to assess the risk of indoor airborne disease transmission.

Our transmission theory and safety guideline provide a quantitative basis for the use of CO_2 monitors in assessing the risk of indoor airborne disease transmission. Specifically, the simple guideline, (5), and mathematical formulae connecting CO_2 data to the evolving transmission risk, (19)–(20), pave the way for real-time assessment of personal risk in indoor spaces. Our safety guideline might also be implemented in spaces where not only CO_2 is monitored, but also other relevant model parameters. For example, changes in occupancy could be monitored at entrances and exits, while monitoring decibel levels and type of vocalization would serve to inform the infectious aerosol production rate (Asadi et al., 2019, 2020c; Morawska et al., 2009). One could further envision feeding all such data into air regulation controls in order to ensure that our CO_2-based indoor safety limit is never violated. We note that such a prospect would be most easily achieved in quasi-steady circumstances in which a fixed population is behaving in a predictable fashion over the course of an event of known duration, for example, students in a lecture hall or passengers on a charter bus. In more complicated situations, our model provides a framework for optimizing sensor-based, demand-controlled ventilation (Fisk & De Almeida, 1998), with a view to limiting transmission risk while reducing energy consumption and system costs (Risbeck et al. 2021a, 2021b). Finally, our model provides a general framework for using CO_2 monitors to mitigate the indoor airborne transmission of other respiratory illnesses, including the seasonal flu.

In order to facilitate the application of our safety guideline, in the supplementary material we provide a link to an online app that computes the safety guideline in terms of both room occupancy and CO_2

https://doi.org/10.1017/flo.2021.10 Published online by Cambridge University Press

levels (Khan et al., 2020). The CO_2-based guideline, available in the app's advanced mode, may be used in conjunction with CO_2 monitors to formulate safe reopening strategies for indoor spaces in the later stages of the pandemic.

Acknowledgements. We thank L. Champion for valuable discussions and for sharing preliminary data and Roberto Rondanelli for references.

Funding Statement. The authors received no funding for this work.

Declaration of Interests. The authors report no conflict of interest.

Data Availability Statement. Raw data are available from M.Z.B. and O.K.

Ethical Standards. The research meets all ethical guidelines, including adherence to the legal requirements of the study country.

Supplementary Material. Supplementary material are available at https://indoor-covid-safety.herokuapp.com.

References

Abdool Karim, S. S., & de Oliveira, T. (2021). New SARS-CoV-2 variants–clinical, public health, and vaccine implications. *New England Journal of Medicine*, *384*(19), 1866–1868.

Abkarian, M., Mendez, S., Xue, N., Yang, F., & Stone, H. A. (2020a). Puff trains in speaking produce long-range turbulent jet-like transport potentially relevant to asymptomatic spreading of viruses. Advance online publication. arXiv:2006.10671.

Abkarian, M., Mendez, S., Xue, N., Yang, F., & Stone, H. A. (2020b). Speech can produce jet-like transport relevant to asymptomatic spreading of virus. *Proceedings of the National Academy of Sciences*, *117*(41), 25237.

Abkarian, M., & Stone, H. (2020). Stretching and break-up of saliva filaments during speech: A route for pathogen aerosolization and its potential mitigation. *Physical Review Fluids*, *5*(10), 102301.

Asadi, S., Bouvier, N., Wexler, A. S., & Ristenpart, W. D. (2020a). The coronavirus pandemic and aerosols: Does COVID-19 transmit via expiratory particles? *Aerosol Science and Technology*, *54*(6), 635–638.

Asadi, S., Cappa, C. D., Barreda, S., Wexler, A. S., Bouvier, N. M., & Ristenpart, W. D. (2020b). Efficacy of masks and face coverings in controlling outward aerosol particle emission from expiratory activities. *Scientific Reports*, *10*(1), 1–13.

Asadi, S., Wexler, A. S., Cappa, C. D., Barreda, S., Bouvier, N. M., & Ristenpart, W. D. (2019). Aerosol emission and superemission during human speech increase with voice loudness. *Scientific Reports*, *9*(1), 1–10.

Asadi, S., Wexler, A. S., Cappa, C. D., Barreda, S., Bouvier, N. M., & Ristenpart, W. D. (2020c). Effect of voicing and articulation manner on aerosol particle emission during human speech. *PLoS ONE*, *15*(1), e0227699.

Augenbraun, B. L., Lasner, Z. D., Mitra, D., Prabhu, S., Raval, S., Sawaoka, H., & Doyle, J. M. (2020). Assessment and mitigation of aerosol airborne SARS-CoV-2 transmission in laboratory and office environments. *Journal of Occupational and Environmental Hygiene*, *17*(10), 447–456.

Bazant, M. Z., & Bush, J. W. M. (2021). A guideline to limit indoor airborne transmission of COVID-19. *Proceedings of the National Academy of Sciences of the United States of America*, *118*(17), e2018995118.

Beggs, C., Noakes, C., Sleigh, P., Fletcher, L., & Siddiqi, K. (2003). The transmission of tuberculosis in confined spaces: An analytical review of alternative epidemiological models. *International Journal of Tuberculosis and Lung Disease*, *7*(11), 1015–1026.

Bhagat, R. K., Wykes, M. D., Dalziel, S. B., & Linden, P. (2020). Effects of ventilation on the indoor spread of COVID-19. *Journal of Fluid Mechanics*, *903*, F1.

Bourouiba, L., Dehandschoewercker, E., & Bush, J. W. M. (2014). Violent expiratory events: On coughing and sneezing. *Journal of Fluid Mechanics*, *745*, 537–563.

Bueno de Mesquita, P. J., Noakes, C. J., & Milton, D. K. (2020). Quantitative aerobiologic analysis of an influenza human challenge-transmission trial. *Indoor Air*, *30*(6), 1189–1198.

Buonanno, G., Morawska, L., & Stabile, L. (2020a). Quantitative assessment of the risk of airborne transmission of SARS-CoV-2 infection. *Environment International*, *145*, 106112.

Buonanno, G., Stabile, L., & Morawska, L. (2020b). Estimation of airborne viral emission: Quanta emission rate of SARS-CoV-2 for infection risk assessment. *Environment International*, *141*, 105794.

Chen, C.-C., & Willeke, K. (1992). Aerosol penetration through surgical masks. *American Journal of Infection Control*, *20*(4), 177–184.

Chen, N., Zhou, M., Dong, X., Qu, J., Gong, F., Han, Y., . . . Zhang, L. (2020). Epidemiological and clinical characteristics of 99 cases of 2019 novel coronavirus pneumonia in Wuhan, China: A descriptive study. *The Lancet*, *395*(10223), 507–513.

Cheng, K.-C., Acevedo-Bolton, V., Jiang, R.-T., Klepeis, N. E., Ott, W. R., Fringer, O. B., & Hildemann, L. M. (2011). Modeling exposure close to air pollution sources in naturally ventilated residences: Association of turbulent diffusion coefficient with air change rate. *Environmental Science & Technology*, *45*(9), 4016–4022.

Coley, D. A., Greeves, R., & Saxby, B. K. (2007). The effect of low ventilation rates on the cognitive function of a primary school class. *International Journal of Ventilation*, *6*(2), 107–112.

Corner, J., & Pendlebury, E. (1951). The coagulation and deposition of a stirred aerosol. *Proceedings of the Physical Society. Section B*, *64*(8), 645.

Corsi, R., Torres, V., Sanders, M., & Kinney, K. (2002). Carbon dioxide levels and dynamics in elementary schools: Results of the Tesias study. *Indoor Air*, *2*, 74–79.

Davies, N. G., Barnard, R. C., Jarvis, C. I., Kucharski, A. J., Munday, J., Pearson, C. A., . . . Edmunds, W. J. (2020). Estimated transmissibility and severity of novel SARS-CoV-2 variant of concern 202012/01 in England. *medRxiv*.

Davis, M. E., & Davis, R. J. (2012). *Fundamentals of chemical reaction engineering*. Courier Corporation. North Chelmsford, MA.

Evans, M. (2020). Avoiding COVID-19: Aerosol guidelines. Advance online publication. arXiv:2005.10988.

Filipić, A., Gutierrez-Aguirre, I., Primc, G., Mozetič, M., & Dobnik, D. (2020). Cold plasma, a new hope in the field of virus inactivation. *Trends in Biotechnology*, *38*, 1278–1291.

Fisk, W. J. (2000). Health and productivity gains from better indoor environments and their relationship with building energy efficiency. *Annual Review of Energy and the Environment*, *25*(1), 537–566.

Fisk, W. J., & De Almeida, A. T. (1998). Sensor-based demand-controlled ventilation: A review. *Energy and Buildings*, *29*(1), 35–45.

Fisk, W. J., Satish, U., Mendell, M. J., Hotchi, T., & Sullivan, D. (2013). Is CO_2 an indoor pollutant? Higher levels of CO_2 may diminish decision making performance. *ASHRAE Journal*, *55*, LBNL-6148E.

Foster, A., & Kinzel, M. (2021). Estimating COVID-19 exposure in a classroom setting: A comparison between mathematical and numerical models. *Physics of Fluids*, *33*(2), 021904.

Gammaitoni, L., & Nucci, M. C. (1997). Using a mathematical model to evaluate the efficacy of TB control measures. *Emerging Infectious Diseases*, *3*(3), 335.

Gandhi, M., Yokoe, D. S., & Havlir, D. V. (2020). Asymptomatic transmission, the Achilles' heel of current strategies to control COVID-19. *New England Journal of Medicine*, *328*(22), 2158–2160.

García de Abajo, F. J., Hernández, R. J., Kaminer, I., Meyerhans, A., Rosell-Llompart, J., & Sanchez-Elsner, T. (2020). Back to normal: An old physics route to reduce SARS-CoV-2 transmission in indoor spaces. *ACS Nano*, *14*(7), 7704–7713.

Garg, S. (2020). Hospitalization rates and characteristics of patients hospitalized with laboratory-confirmed coronavirus disease 2019: COVID-NET, 14 States, March 1–30, 2020. *MMWR. Morbidity and Mortality Weekly Report*, *69*(15), 458–464.

Gettings, J., Czarnik, M., Morris, E., Haller, E., Thompson-Paul, A. M., Rasberry, C., . . . MacKellar, D. (2021). Mask use and ventilation improvements to reduce COVID-19 incidence in elementary schools–Georgia, November 16–December 11, 2020. *MMWR. Morbidity and Mortality Weekly Report*, *70*, 779–784.

Greenhalgh, T., Jimenez, J. L., Prather, K. A., Tufekci, Z., Fisman, D., & Schooley, R. (2021). Ten scientific reasons in support of airborne transmission of SARS-CoV-2. *The Lancet*, *397*(10285), 1603–1605.

Hamner, L. (2020). High SARS-CoV-2 attack rate following exposure at a choir practice, Skagit County, Washington, March 2020. *MMWR. Morbidity and Mortality Weekly Report*, *69*(19), 606–610.

Hartmann, A., & Kriegel, M. (2020). Risk assessment of aerosols loaded with virus based on co2-concentration. Advance online publication. doi:10.14279/depositonce-10362.3.

Higuchi, K., Worthy, D., Chan, D., & Shashkov, A. (2003). Regional source/sink impact on the diurnal, seasonal and inter-annual variations in atmospheric CO_2 at a boreal forest site in Canada. *Tellus B: Chemical and Physical Meteorology*, *55*(2), 115–125.

Hitchman, M. L. (2021). A new perspective of the chemistry and kinetics of inactivation of COVID-19 coronavirus aerosols. *Future Virology*, *15*(12), 823–835.

Hung, I.-F., & Derossis, P. (1989). Carbon dioxide concentration as indicator of indoor air quality. *Journal of Environmental Science and Health. Part A: Environmental Science and Engineering*, *24*(4), 379–388.

Hwang, S. E., Chang, J. H., Bumjo, O., & Heo, J. (2020). Possible aerosol transmission of COVID-19 associated with an outbreak in an apartment in Seoul, South Korea. *International Journal of Infectious Diseases*. *104*, 73–76.

Jayaweera, M., Perera, H., Gunawardana, B., & Manatunge, J. (2020). Transmission of COVID-19 virus by droplets and aerosols. *Environmental Research*, *188*, 109819.

Khan, K., Bazant, M. Z., & Bush, J. W. M. (2020). COVID-19 indoor safety guideline. [Mobile application software]. Retrieved from https://indoor-covid-safety.herokuapp.com.

Konda, A., Prakash, A., Moss, G. A., Schmoldt, M., Grant, G. D., & Guha, S. (2020a). Aerosol filtration efficiency of common fabrics used in respiratory cloth masks. *ACS Nano*, *14*(5), 6339–6347.

Konda, A., Prakash, A., Moss, G. A., Schmoldt, M., Grant, G. D., & Guha, S. (2020b). Response to letters to the editor on aerosol filtration efficiency of common fabrics used in respiratory cloth masks: Revised and expanded results. *ACS Nano*, *14*(9), 10764–10770.

Krawczyk, D., Rodero, A., Gładyszewska-Fiedoruk, K., & Gajewski, A. (2016). CO_2 concentration in naturally ventilated classrooms located in different climates—measurements and simulations. *Energy and Buildings*, *129*, 491–498.

Kwon, K.-S., Park, J.-I., Park, Y. J., Jung, D.-M., Ryu, K.-W., & Lee, J.-H. (2020). Evidence of long-distance droplet transmission of SARS-CoV-2 by direct air flow in a restaurant in Korea. *Journal of Korean Medical Science*, *35*(46), e415.

Lai, A., Cheung, A., Wong, M., & Li, W. (2016). Evaluation of cold plasma inactivation efficacy against different airborne bacteria in ventilation duct flow. *Building and Environment*, *98*, 39–46.

Lednicky, J. A., Lauzard, M., Fan, Z. H., Jutla, A., Tilly, T. B., Gangwar, M., . . . Wu, C. (2020). Viable SARS-CoV-2 in the air of a hospital room with COVID-19 patients. *International Journal of Infectious Diseases*, *100*, 476–482.

https://doi.org/10.1017/flo.2021.10 Published online by Cambridge University Press

Lewis, D. (2021). Covid-19 rarely spreads through surfaces. So why are we still deep cleaning. *Nature*, *590*(7844), 26–28.
Li, Q., Guan, X., Wu, P., Wang, X., Zhou, L., Tong, Y., . . . Feng, Z. (2020). Early transmission dynamics in Wuhan, China, of novel coronavirus–infected pneumonia. *New England Journal of Medicine*, *382*, 1199–1207.
Li, Y., Guo, Y. P., Wong, K. C. T., Chung, W. Y. J., Gohel, M. D. I., & Leung, H. M. P. (2008). Transmission of communicable respiratory infections and facemasks. *Journal of Multidisciplinary Healthcare*, *1*, 17.
Li, Y., Leung, G. M., Tang, J., Yang, X., Chao, C., Lin, J. Z., . . . Yuen, P.L. (2007). Role of ventilation in airborne transmission of infectious agents in the built environment-a multidisciplinary systematic review. *Indoor Air*, *17*(1), 2–18.
Lin, K., & Marr, L. C. (2019). Humidity-dependent decay of viruses, but not bacteria, in aerosols and droplets follows disinfection kinetics. *Environmental Science & Technology*, *54*(2), 1024–1032.
Linden, P., Lane-Serff, G., & Smeed, D. (1990). Emptying filling boxes: The fluid mechanics of natural ventilation. *Journal of Fluid Mechanics*, *212*, 309–335.
Linden, P. F. (1999). The fluid mechanics of natural ventilation. *Annual Review of Fluid Mechanics*, *31*(1), 201–238.
Liu, L.-J. S., Krahmer, M., Fox, A., Feigley, C. E., Featherstone, A., Saraf, A., & Larsson, L. (2000). Investigation of the concentration of bacteria and their cell envelope components in indoor air in two elementary schools. *Journal of the Air & Waste Management Association*, *50*(11), 1957–1967.
MacNaughton, P., Pegues, J., Satish, U., Santanam, S., Spengler, J., & Allen, J. (2015). Economic, environmental and health implications of enhanced ventilation in office buildings. *International Journal of Environmental Research and Public Health*, *12*(11), 14709–14722.
Marr, L. C., Tang, J. W., Van Mullekom, J., & Lakdawala, S. S. (2019). Mechanistic insights into the effect of humidity on airborne influenza virus survival, transmission and incidence. *Journal of the Royal Society Interface*, *16*(150), 20180298.
Martin, D., & Nokes, R. (1988). Crystal settling in a vigorously converting magma chamber. *Nature*, *332*(6164), 534–536.
Mendell, M. J., Eliseeva, E. A., Davies, M. M., Spears, M., Lobscheid, A., Fisk, W. J., & Apte, M. G. (2013). Association of classroom ventilation with reduced illness absence: A prospective study in California elementary schools. *Indoor Air*, *23*(6), 515–528.
Miller, S. L., Nazaroff, W. W., Jimenez, J. L., Boerstra, A., Buonanno, G., Dancer, S. J., . . . Noakes, C. (2020). Transmission of SARS-CoV-2 by inhalation of respiratory aerosol in the Skagit Valley Chorale superspreading event. *Indoor Air*, *31*(2), 314–323.
Milton, D. K., Glencross, P. M., & Walters, M. D. (2000). Risk of sick leave associated with outdoor air supply rate, humidification, and occupant complaints. *Indoor Air*, *10*(4), 212–221.
Moghadas, S. M., Fitzpatrick, M. C., Sah, P., Pandey, A., Shoukat, A., Singer, B. H., & Galvani, A. P. (2020). The implications of silent transmission for the control of COVID-19 outbreaks. *Proceedings of the National Academy of Sciences*, *117*(30), 17513–17515.
Morawska, L., Allen, J., Bahnfleth, W., Bluyssen, P. M., Boerstra, A., Buonanno, G., . . . Yao, M. (2021). A paradigm shift to combat indoor respiratory infection. *Science*, *372*(6543), 689–691.
Morawska, L., & Cao, J. (2020). Airborne transmission of SARS-CoV-2: The world should face the reality. *Environment International*, *139*, 105730.
Morawska, L., Johnson, G., Ristovski, Z., Hargreaves, M., Mengersen, K., Corbett, S., . . . Katoshevski, D. (2009). Size distribution and sites of origin of droplets expelled from the human respiratory tract during expiratory activities. *Journal of Aerosol Science*, *40*, 256–269.
Morawska, L., & Milton, D. K. (2020). It is time to address airborne transmission of COVID-19. *Clinical Infectious Diseases*, *71*, 2311–2313.
Moriarty, L. F. (2020). Public health responses to COVID-19 outbreaks on cruise ships worldwide, February–March 2020. *MMWR. Morbidity and Mortality Weekly Report*, *69*(12), 347–352.
Nasreen, S., He, S., Chung, H., Brown, K.A., Gubbay, J.B., Buchan, S.A., . . . Kwong, J.C. (2021). Effectiveness of COVID-19 vaccines against variants of concern, Canada. medRxiv. doi:10.1101/2021.06.28.21259420.
Nicas, M., Nazaroff, W. W., & Hubbard, A. (2005). Toward understanding the risk of secondary airborne infection: Emission of respirable pathogens. *Journal of Occupational and Environmental Hygiene*, *2*(3), 143–154.
Nishiura, H., Oshitani, H., Kobayashi, T., Saito, T., Sunagawa, T., Matsui, T., . . . Suzuki, M. (2020). Closed environments facilitate secondary transmission of coronavirus disease 2019 (COVID-19). Advance online publication. doi:10.1101/2020.02.28.20029272.
Noakes, C., Beggs, C., Sleigh, P., & Kerr, K. (2006). Modelling the transmission of airborne infections in enclosed spaces. *Epidemiology & Infection*, *134*(5), 1082–1091.
Noakes, C. J., & Sleigh, P. A. (2009). Mathematical models for assessing the role of airflow on the risk of airborne infection in hospital wards. *Journal of the Royal Society Interface*, *6*(suppl_6), S791–S800.
Oberg, T., & Brosseau, L. M. (2008). Surgical mask filter and fit performance. *American Journal of Infection Control*, *36*(4), 276–282.
Pan, J., Harb, C., Leng, W., & Marr, L. C. (2020). Inward and outward effectiveness of cloth masks, a surgical mask, and a face shield. Advance online publication. doi:10.1101/2020.11.18.20233353.
Peng, Z., & Jimenez, J. L. (2021). Exhaled CO_2 as COVID-19 infection risk proxy for different indoor environments and activities. *Environmental Science and Technology Letters*. *8*, 392–397.

https://doi.org/10.1017/flo.2021.10 Published online by Cambridge University Press

Persily, A., & de Jonge, L. (2017). Carbon dioxide generation rates for building occupants. *Indoor Air*, *27*(5), 868–879.
Prather, K. A., Marr, L. C., Schooley, R. T., McDiarmid, M. A., Wilson, M. E., & Milton, D. K. (2020). Airborne transmission of SARS-CoV-2. *Science*, *370*(6514), 303–304.
Prentiss, M. G., Chu, A., & Berggren, K. K. (2020). Superspreading events without superspreaders: Using high attack rate events to estimate n_o for airborne transmission of COVID-19. Advance online publication. doi:10.1101/2020.10.21.20216895.
Prill, R. (2000). Why measure carbon dioxide inside buildings. *Published by Washington State University Extension Energy Program WSUEEP07*, 3.
Riediker, M., & Morawska, L. (2020). Low exhaled breath droplet formation may explain why children are poor SARS-CoV-2 transmitters. *Aerosol and Air Quality Research*, *20*(7), 1513–1515.
Riley, E. C., Murphy, G., & Riley, R. L. (1978). Airborne spread of measles in a suburban elementary school. *American Journal of Epidemiology*, *107*(5), 421–432.
Risbeck, M.J., Bazant, M.Z., Jiang, Z., Lee, Y.M., Drees, K.H., & Douglas, J.D. (2021a). Quantifying the tradeoff between energy consumption and the risk of airborne disease transmission for building HVAC systems. Advance online publication. doi:10.1101/2021.06.21.21259287.
Risbeck, M.J., Bazant, M.Z., Jiang, Z., Lee, Y.M., Drees, K.H., & Douglas, J.D. (2021b). Modeling and multiobjective optimization of indoor airborne disease transmission risk and associated energy consumption for building HVAC systems. Advance online publication. doi:10.1101/2021.08.10.21261866.
Rosti, M., Olivieri, S., Cavaiola, M., Seminara, A., & Mazzino, A. (2020). Fluid dynamics of COVID-19 airborne infection suggests urgent data for a scientific design of social distancing. *Scientific Reports*, *10*(1), 1–9.
Rudnick, S., & Milton, D. (2003). Risk of indoor airborne infection transmission estimated from carbon dioxide concentration. *Indoor Air*, *13*(3), 237–245.
Salisbury, S. (1986). Measuring carbon dioxide levels as an indicator of poor building ventilation: A case study. In *Proc. IAQ'86* (pp. 78–82).
Santarpia, J. L., Herrera, V. L., Rivera, D. N., Ratnesar-Shumate, S., Reid, S., Denton, P. W., . . . Lowe, J. J. (2020). The infectious nature of patient-generated SARS-CoV-2 aerosol. Advance online publication. doi:10.1101/2020.07.13.20041632.
Schwartz, A., Stiegel, M., Greeson, N., Vogel, A., Thomann, W., Brown, M., . . . Lewis, S. (2020). Decontamination and reuse of N95 respirators with hydrogen peroxide vapor to address worldwide personal protective equipment shortages during the SARS-CoV-2 (COVID-19) pandemic. *Applied Biosafety*, *25*(2), 67–70.
Seppänen, O., Fisk, W., & Mendell, M. (1999). Association of ventilation rates and CO_2 concentrations with health and other responses in commercial and institutional buildings. *Indoor Air*, *9*(4), 226–252.
Shair, F. H., & Heitner, K. L. (1974). Theoretical model for relating indoor pollutant concentrations to those outside. *Environmental Science & Technology*, *8*(5), 444–451.
Sheikh, A., McMenamin, J., Taylor, R., & Robertson, C. (2021). Public Health Scotland and the EAVE II Collaborators. SARS-CoV-2 delta VOC in Scotland: demographics, risk of hospital admission, and vaccine effectiveness. *Lancet*, *397*, 2461–2462.
Shen, Y., Li, C., Dong, H., Wang, Z., Martinez, L., Sun, Z., . . . Xu, G. (2020). Community outbreak investigation of SARS-CoV-2 transmission among bus riders in eastern China. *JAMA Internal Medicine*, *180*(12), 1665–1671.
Shendell, D. G., Prill, R., Fisk, W. J., Apte, M. G., Blake, D., & Faulkner, D. (2004). Associations between classroom CO_2 concentrations and student attendance in Washington and Idaho. *Indoor Air*, *14*(5), 333–341.
Stadnytskyi, V., Bax, C. E., Bax, A., & Anfinrud, P. (2020). The airborne lifetime of small speech droplets and their potential importance in SARS-CoV-2 transmission. *Proceedings of the National Academy of Sciences*, *117*(22), 11875–11877.
Stilianakis, N. I., & Drossinos, Y. (2010). Dynamics of infectious disease transmission by inhalable respiratory droplets. *Journal of the Royal Society Interface*, *7*(50), 1355–1366.
Stutt, R. O. J. H., Retkute, R., Bradley, M., Gilligan, C. A., & Colvin, J. (2020). A modelling framework to assess the likely effectiveness of facemasks in combination with lock-down in managing the COVID-19 pandemic. *Proceedings of the Royal Society A*, *476*, 20200376.
Sun, Y., Wang, Z., Zhang, Y., & Sundell, J. (2011). In China, students in crowded dormitories with a low ventilation rate have more common colds: Evidence for airborne transmission. *PLoS ONE*, *6*(11), e27140.
Tang, J. W., Bahnfleth, W. P., Bluyssen, P. M., Buonanno, G., Jimenez, J. L., Kurnitski, J., . . . Dancer, S. J. (2021). Dismantling myths on the airborne transmission of severe acute respiratory syndrome coronavirus (SARS-CoV-2). *Journal of Hospital Infection*, *84*, 271–282.
van den Berg, P., Schechter-Perkins, E. M., Jack, R. S., Epshtein, I., Nelson, R., Oster, E., & Branch-Elliman, W. (2021). Effectiveness of three versus six feet of physical distancing for controlling spread of COVID-19 among primary and secondary students and staff: A retrospective, state-wide cohort study. *Clinical Infectious Diseases*, ciab230.
Van Doremalen, N., Bushmaker, T., Morris, D. H., Holbrook, M. G., Gamble, A., Williamson, B. N., . . . Munster, V. J. (2020). Aerosol and surface stability of SARS-CoV-2 as compared with SARS-CoV-1. *New England Journal of Medicine*, *382*(16), 1564–1567.
Volz, E., Mishra, S., Chand, M., Barrett, J. C., Johnson, R., Geidelberg, L., . . . Ferguson, N. M. (2021). Transmission of SARS-CoV-2 lineage B.1.1.7 in England: Insights from linking epidemiological and genetic data. Advance online publication. doi:10.1101/2020.12.30.20249034.

Watanabe, T., Bartrand, T. A., Weir, M. H., Omura, T., & Haas, C. N. (2010). Development of a dose-response model for SARS coronavirus. *Risk Analysis*, *30*(7), 1129–1138.

Wells, W. F. (1955). *Airborne contagion and air hygiene: An ecological study of droplet infections*. Cambridge, MA: Harvard University Press.

Yang, W., & Marr, L. C. (2011). Dynamics of airborne influenza A viruses indoors and dependence on humidity. *PLoS ONE*, *6*(6), 1–10.

Zhang, J., Litvinova, M., Liang, Y., Wang, Y., Wang, W., Zhao, S., . . . Yu, H. (2020a). Changes in contact patterns shape the dynamics of the COVID-19 outbreak in China. *Science*, *368*, 1481–1486.

Zhang, R., Li, Y., Zhang, A. L., Wang, Y., & Molina, M. J. (2020b). Identifying airborne transmission as the dominant route for the spread of COVID-19. *Proceedings of the National Academy of Sciences of the United States of America*, *117*(26), 14857–14863.

Zhu, Y., Bloxham, C. J., Hulme, K. D., Sinclair, J. E., Tong, Z. W. M., Steele, L. E., . . . Short, K. R. (2020). A meta-analysis on the role of children in SARS-CoV-2 in household transmission clusters. *Clinical Infectious Diseases*. *72*, e1146–e1153.

Cite this article: Bazant MZ, Kodio O, Cohen AE, Khan K, Gu Z & Bush JWM (2021). Monitoring carbon dioxide to quantify the risk of indoor airborne transmission of COVID-19. *Flow*, *1*, E10. doi:10.1017/flo.2021.10